research articles Journal of proteome research

Effect of Zinc and Temperature on the Conformation of the γ Subunit of Retinal Phosphodiesterase: A Natively Unfolded Protein

Vladimir N. Uversky,*,†,‡ Sergey E. Permyakov,† Vasily E. Zagranichny,§ Igor L. Rodionov,§ Anthony L. Fink,‡ Alexandra M. Cherskaya,† Lyubov A.Wasserman,|| and Eugene A. Permyakov†

Institute for Biological Instrumentation, Russian Academy of Sciences, 142290 Pushchino, Moscow Region, Russia, Department of Chemistry and Biochemistry, University of California, Santa Cruz, California 95064, Branch of M. M. Shemyakin and Yu. A. Ovchinnikov Institute of Bioorganic Chemistry, Russian Academy of Sciences, 142290 Pushchino, Moscow Region, Russia, and Institute of Biochemical Physics, Russian Academy of Sciences, 4 Kosygin Str., 117334 Moscow, Russia

Received November 29, 2001

The cyclic GMP phosphodiesterase γ-subunit (PDEγ) was shown to belong to the family of natively unfolded proteins. Increasing temperature transforms the protein into a more ordered (but still relatively disordered) conformation. The C-terminal part of PDEγ has a high-affinity zinc-binding site ($K_d \sim 1\ \mu M$), with His75 and His79 being directly involved into the coordination of Zn^{2+}. Zinc-loaded protein remains effectively unfolded. Possible implications of these findings to the functioning of PDEγ are discussed.

Keywords: cyclic GMP phosphodiesterase • signal transduction • intrinsically unordered protein • conformational transition • partially folded intermediate

Introduction

cGMP phosphodiesterase (PDE) from retinal rods plays a key role in the process of visual signal transduction (reviewed in ref 1) catalyzing conversion of cyclic GMP into GMP. The PDE holoenzyme is a functionally inactive heterotetramer of $\alpha\beta\gamma_2$ composition. The catalytically active dimer of two large homologous α- and β-subunits is reversibly inhibited by small γ-subunit, PDEγ.[2] PDE activation in the course of visual signal amplification results from the interaction of PDE with the α-subunit of photoreceptor-specific G-protein, transducin, which is, in its turn, activated by photoexcited rhodopsin.[3,4] In the GTP-bound state, the α-subunit of transducin acquires a high affinity for PDEγ due to a GTP-induced conformational rearrangement. This affinity is lost after hydrolysis of the GTP.[3]

It is widely accepted that the retina is characterized by an elevated level of zinc cations in comparison with the majority of other soft tissues.[5] Data on the exact zinc concentrations in photoreceptor cell cytoplasm are contradictory (see, for example, refs 6−8). Little is currently known about the possible role of this cation in photoreceptor functioning. Zinc was believed to be bound to retinol dehydrogenase[7] and was also shown to exist in a complex with rhodopsin.[8] We have established previously that PDEγ binds zinc.[9] In the present paper, the problem of zinc interaction with PDEγ will be considered in more detail.

The number of proteins and protein domains that have been shown to have little or no ordered structure under physiological conditions has increased rapidly over the past 10 years. The special term "natively unfolded" has been introduced as a descriptive appellation for such proteins.[10,11] Natively unfolded or intrinsically unstructured proteins occupy a unique niche within the protein kingdom in that they are disordered under conditions of neutral pH in vitro yet nevertheless possess marked biological activities. Analysis of amino acid sequences, based on the normalized net charge and mean hydrophobicity, shows that these proteins are specifically localized within a unique region of charge−hydrophobicity phase space, thus possessing a unique structural feature, a combination of low overall hydrophobicity and large net charge.[12]

It has been suggested that the lack of rigid globular structure under physiological conditions might represent a considerable functional advantage for natively unfolded proteins, as their large plasticity allows them to interact efficiently with several different targets.[13,14] Moreover, a disorder−order transition induced in intrinsically disordered proteins during the binding to their specific targets in vivo might represent a simple mechanism for regulation of numerous cellular processes, including transcriptional and translational regulation and cell cycle control.[13,14] Evolutionary persistence of the natively unfolded proteins provides an additional confirmation of their importance and raises intriguing questions on the role of protein disorder in biological processes.

We have found that PDEγ is a natively unstructured protein. Here, we represent a detailed study of PDEγ structural proper-

* To whom correspondence should be addressed at the University of California. Tel: 831-459-2915. Fax: 831-459-2935. E-mail: uversky@hydrogen.ucsc.edu.

† Institute for Biological Instrumentation, Russian Academy of Sciences.

‡ University of California.

§ Branch of M. M. Shemyakin and Yu. A. Ovchinnikov Institute of Bioorganic Chemistry, Russian Academy of Sciences.

|| Institute of Biochemical Physics, Russian Academy of Sciences.

10.1021/pr0155127 CCC: $22.00

Published on Web 02/06/2002

ties under physiological conditions and describe the effect of zinc cations on the structural and conformational properties of this protein.

Experimental Section

Materials. All chemicals were the highest grade available. Solutions were prepared with double-distilled, deionized water. Protein concentrations were evaluated spectrophotometrically using an extinction coefficient of $\epsilon_{280} = 6970\ M^{-1}\ cm^{-1}$, which was calculated on the basis of the PDEγ amino acid composition.

PDEγ Expression and Isolation. The *E. coli* cells, strain BL22(DE3), were transformed with the plasmid (a pET11a derivative) encoding PDEγ.[15] A single colony was grown overnight at 37 °C in the presence of 50 μg/mL carbenicillin. The overnight culture was diluted 1:200 into SM (12 g of tryptone, 24 g of yeast extract, 1 mL of 1 M NaOH, per liter) containing 50 μg/mL of carbenicillin and grown at 37 °C. At an optical density of ~1.0 (at 600 nm), protein expression was induced by the addition of 1 mM IPTG. Upon induction, the temperature was reduced to 30 °C and the cells were grown for another 5 h. The cells were spun down, resuspended in 1/40 volume sonication buffer (50 mM Tris-HCl pH7.5, 2 mM EDTA, 50 mM NaCl, 1 mM DTT, 20 μg/mL of pepstatin A, 5 μg/mL of leupeptin, and 1 mM PMSF), and sonicated. Insoluble material was removed by centrifugation for 30 min at 4 °C and 18 000 rpm with a JA-20 rotor (Beckman, J-21). The supernatant was loaded into a Pharmacia Mono-S (HR 5/5) cation-exchange column equilibrated with 50 mM Tris-HCl pH 7.5, 20 mM NaCl, 2 mM EDTA, and 2 mM β-mercaptoethanol. Flow rate was kept at 1 mL/min. Protein was eluted with a NaCl gradient (20 mM to 1 M), with the major PDEγ peak eluting at ~400 mM NaCl. Fractions containing PDEγ were loaded onto a Synchropak C-4 (6.6 μm) reversed-phase HPLC column equilibrated with 0.01% TFA. An acetonitrile gradient (from 0 to 70%) was used to elute PDEγ (30% solvent). The PDEγ-containing fraction was lyophilized and further characterized by N-terminal sequencing and mass spectrometry (MALDI). The PDEγ purity was no less than 98% according to both these methods.

Truncated PDEγ derivatives were isolated and characterized as described for the full-length protein except lower concentrations of protease inhibitors were used in the sonication buffer. The PDEγ E58-I87 fragment was generated using cyanogen bromide cleavage and isolated as described in ref 2).

Methods. Fluorescence spectra were measured on a Jobin Yvon-Spex spectrofluorimeter. All spectra were corrected for spectral sensitivity of the instrument. Circular dichroism measurements were performed on AVIV 62DS spectropolarimeter. Typical instrument conditions were as follows: scan rate, 5 nm/min; time constant, 8 s. Path length was 0.1 mm for far-UV studies and 5 mm for the near-UV region. Hydrodynamic dimensions (Stokes radii, R_S) of PDEγ were measured by size-exclusion chromatography. Gel-filtration measurements were carried out on a Superose 12 HR 10/30 column using a Pharmacia FPLC apparatus. A set of globular proteins with known R_S values was used.[16,17] In this case, a specific calibration curve, $1000/V$ versus R_S, was used.[16−20] A least-squares analysis was applied to fit the experimental data to generate the calibration curve:

$$1000/V = (0.73 \pm 0.01)R_S + (52.0 \pm 0.4) \quad (1)$$

Hydrodynamic dimensions of a native and completely unfolded globular protein with a molecular mass of 9669 Da were calculated from empirical equations[17]

$$\log(R_S^N) = 0.369 \log(M) - 0.254 \quad (2)$$

$$\log(R_S^U) = 0.533 \log(M) - 0.682 \quad (3)$$

based on intrinsic viscosity data.[21] Here R_S^N and R_S^U are the Stokes radii of native (N) and completely unfolded (U) proteins, respectively, whereas M corresponds to the protein molecular mass.

Results

PDEγ Is a Natively Unfolded Protein. Amino Acid Sequence Analysis. Natively unfolded proteins, with their unique combination of little or no ordered structure under physiological conditions, but with significant biological activities, represent a distinct subdivision of the protein realm. It has been established that a combination of low overall hydrophobicity and large net charge is a specific feature of this protein class.[12] Natively unfolded proteins are specifically localized within a particular region of charge−hydrophobicity phase space, satisfying the following relationship

$$\langle H \rangle \le \langle H \rangle_b = \frac{\langle R \rangle + 1.151}{2.785} \quad (4)$$

where $\langle H \rangle$ and $\langle R \rangle$ are the mean hydrophobicity and the mean net charge of the given protein, respectively, whereas $\langle H \rangle_b$ is the "boundary" mean hydrophobicity value, below which a polypeptide chain with a given $\langle R \rangle$ will be most probably unfolded. The mean hydrophobicity $\langle H \rangle$ is defined as the sum of the normalized hydrophobicities of all residues divided by the number of residues in the polypeptide. The mean net charge $\langle R \rangle$ is defined as the net charge at pH 7.0, divided by the total number of residues. Analysis of the PDEγ amino acid sequence shows that this protein is characterized by $\langle H \rangle = 0.4195$, $\langle R \rangle = 0.0460$, and $\langle H \rangle_b = 0.4298$, thus fulfilling the requirement for natively unfolded proteins, namely that $\langle H \rangle < \langle H \rangle_b$ ($0.4195 < 0.4298$). This prediction that PDEγ should have a low content of ordered structure was confirmed by experimental results.

Tertiary Structure (Near-UV CD Spectrum). Figure 1 A represents the near-UV CD spectrum of PDEγ measured at pH 8 and 37 °C. Native proteins with rigid tertiary structure are characterized by pronounced near-UV CD spectra due to the asymmetric environment of their aromatic amino acid residues. On the other hand, any kind of denaturation (loss of specific tertiary structure) is accompanied by considerable loss in intensity and fine structure of near-UV CD signals. If PDEγ possessed a rigid tertiary structure, one would expect the presence of several characteristic bands in the near-UV CD spectrum, due to the presence of four phenylalanines (F30, F38, F50, and F73), one tyrosine (Y84), and one tryptophan (W70).[2] However, Figure 1A shows the absence of any specific band. This indicates that PDEγ has no rigid tertiary structure, at least in the vicinity of its aromatic amino acid residues.

Secondary Structure (Far-UV CD Spectrum). Figure 1B represents far-UV CD spectra of PDEγ measured under different experimental conditions. At pH 8 and low temperatures (4 °C), the inhibitory subunit of phosphodiesterase is characterized by a far-UV CD spectrum typical of an essentially unfolded polypeptide chain. The same or very similar spectra have been observed for the majority of natively unfolded proteins (see ref 12 for the latest set of such proteins). In contrast, Figure 1B

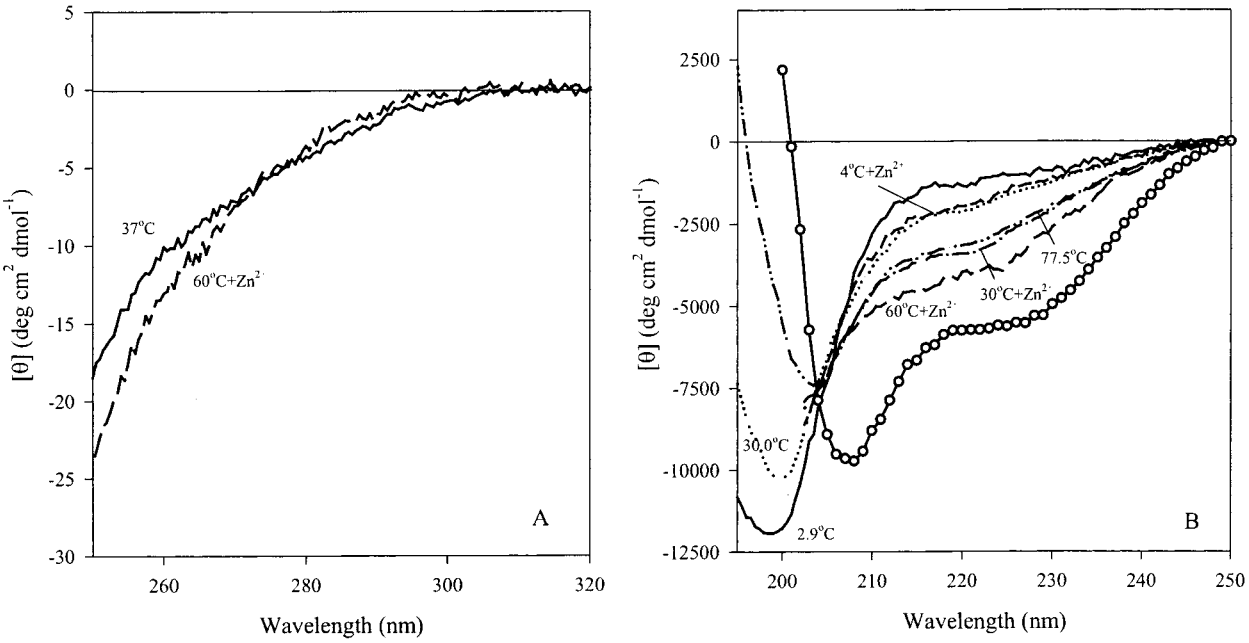

Figure 1. Near-UV (A) and far-UV (B) CD spectra of PDEγ (10 μM) at different temperatures in the presence or absence of zinc. Measurements were carried out in 10 mM HEPES, pH 8.0 buffer. Circles show spectra of the associated form of PDEγ (100 μM). Cell path length was 10 and 0.1 mm for near- and far-UV CD spectra measurements, respectively.

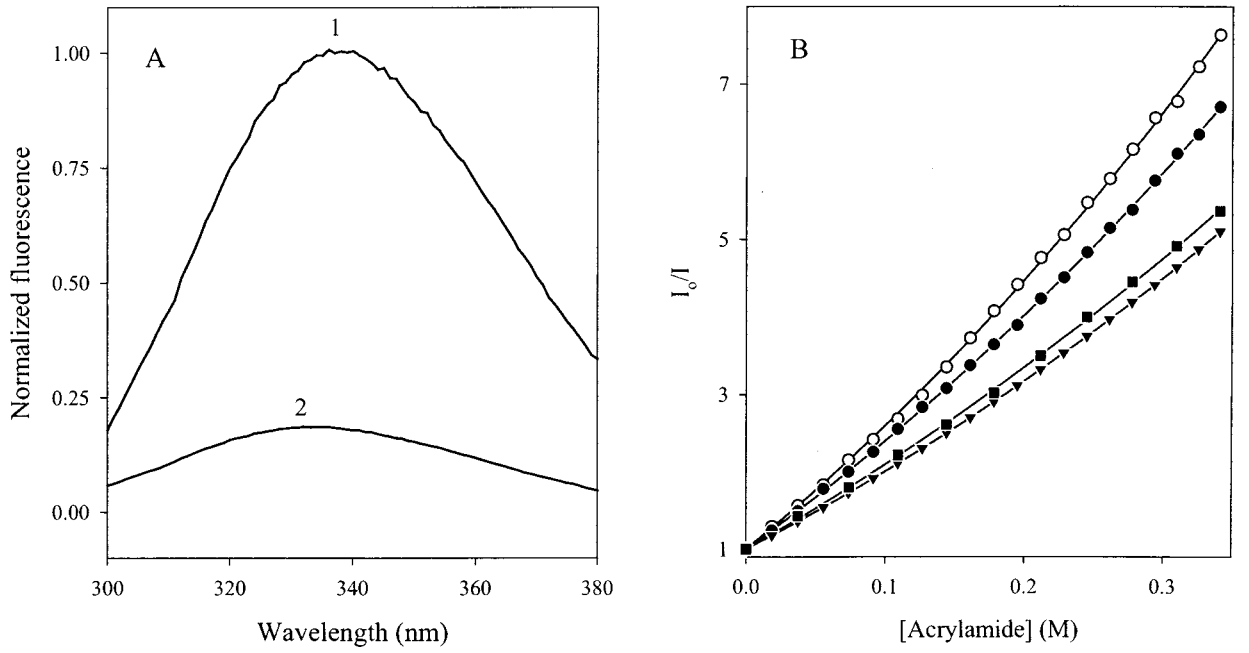

Figure 2. (A) Normalized tryptophan fluorescence spectra of PDEγ (1.14 μM) in the absence (**1**) and in the presence of Zn^{2+} ([Zn^{2+}]/[PDEγ] = 66) (**2**): 10 mM HEPES, pH 8.0; 20 °C. Fluorescence was excited at 280 nm. (B) Stern−Volmer plots for acrylamide quenching of PDEγ tryptophan fluorescence at different temperatures: 3 °C (circles), 30 °C (squares), and 40 °C (triangles). Data for zinc-free and zinc-loaded protein shown by open and black symbols, respectively. Protein concentration was kept ~1 μM. As discussed in the text, the curvature indicates both static and dynamic quenching.

shows that an increase in temperature, or the addition of Zn^{2+}, led to substantial changes in the far-UV CD spectrum, reflecting the existence of considerable structural rearrangement of the protein under these conditions. Structure-forming effects of heating and Zn^{2+} binding will be considered below.

Interestingly, circles in Figure 1 illustrate that at high protein concentrations (~100 μM) PDEγ is characterized by a far-UV CD spectrum typical of a relatively folded protein. On the other hand, control experiments showed that an increase in PDEγ concentration from 1 to 10 μM is not accompanied by any spectral changes (data not shown). This means that the structure of PDEγ is independent of protein concentration within the range of 1−10 μM, whereas further increase in protein content induces PDEγ association and, as a consequence, stabilization of ordered secondary structure.

Intrinsic Fluorescence and Its Acrylamide Quenching. Solvated Trp residues have a fluorescence emission maximum at about 350 nm; while burial of Trp in the nonpolar core of

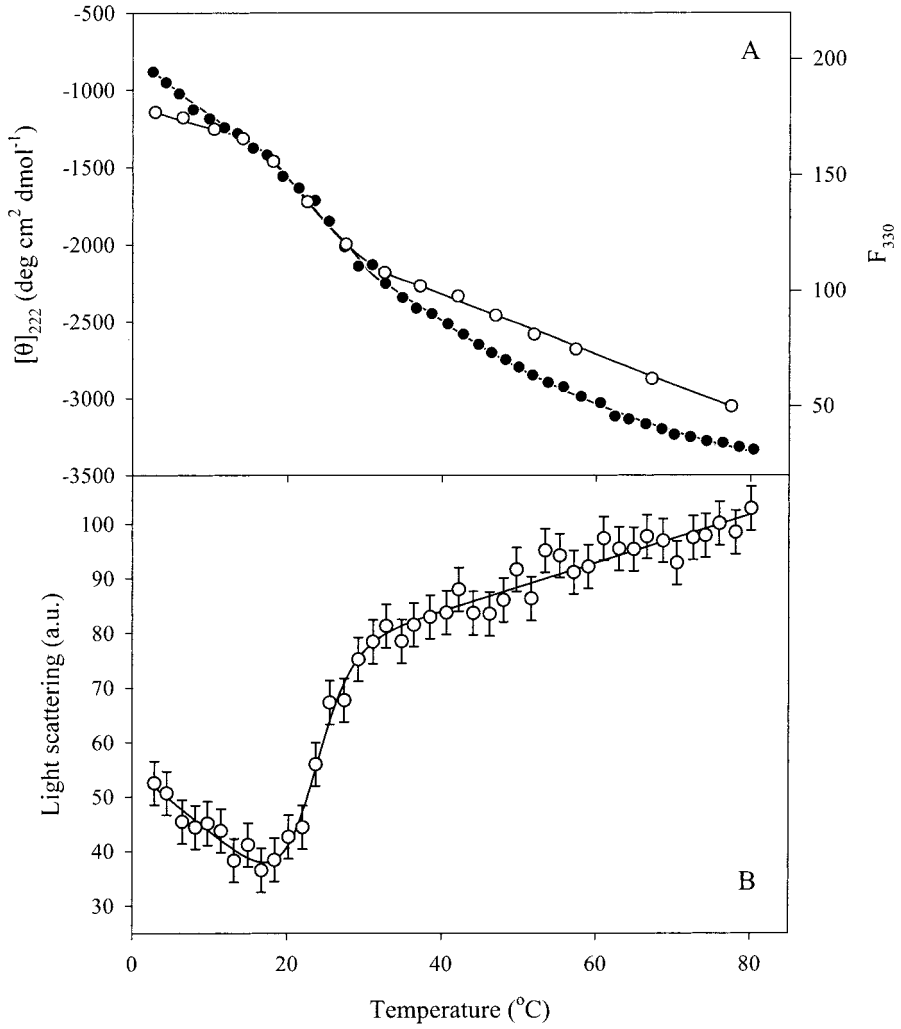

Figure 3. (A) Temperature-induced structural rearrangement of PDEγ monitored by changes in the far-UV CD spectrum ($[\theta]_{222}$, open circles) and intensity of Trp fluorescence spectrum (F_{330}, black circles). Protein concentration was 10 and 1 μM for CD and fluorescence measurements, respectively. (B) Temperature-induced association and dissociation of PDEγ monitored by changes in the static light scattering. Static light-scattering measurements were performed at 330 nm with the excitation at 330 nm. Protein concentration was 1 μM.

globular protein results in a characteristic blue shift of its fluorescence spectrum maximum (in some cases, λ_{max} is as short as 308 nm). Thus, Trp emission spectrum is a sensitive probe of the polarity and mobility of the Trp environment.[22,23] Figure 2A (curve 1) shows the tryptophan fluorescence spectra of PDEγ measured at pH 8.0 and 4 °C. One can see that protein is characterized by the Trp spectrum with λ_{max} ~340 nm. This means that tryptophan residue of PDEγ is relatively solvent-exposed.

Additional information on the relative solvent exposure of tryptophan residues in a protein can be obtained from analysis of the effect of quencher molecules (e.g., acrylamide, see refs 24 and25). Figure 2B represents the Stern−Volmer plots, i.e., dependency of I_o/I on acrylamide concentration (where I_o and I are the Trp fluorescence intensities in the absence and presence of quencher, respectively), for PDEγ under different experimental conditions. The Stern−Volmer plot is usually linear when the fluorescence involves dynamic or collision quenching. The upward curvature of such dependence (as observed in this case, see Figure 2B) indicates the presence of an additional quenching process, static quenching.[24,25] To account for this curvature, data on the acrylamide quenching of Trp fluorescence were analyzed according to the general form of the Stern−Volmer equation, which takes into account both quenching mechanisms

$$\frac{I_o}{I} = (1 + K_{SV}[Q])e^{V[Q]} \quad (5)$$

where I_o and I are the fluorescence intensities in the absence and presence of quencher, K_{SV} is the dynamic quenching constant, V is the static quenching constant, and $[Q]$ is the total quencher concentration. Although both the dynamic (K_{SV}) and the static (V) quenching constants provide information concerning the accessibility of the Trp residue to quencher molecules, it has been observed that the V values are much less reproducible than K_{SV} values.[24,25] Thus, only the values of K_{SV} will be considered here. The results of this analysis show that under conditions of neutral pH and low temperature $K_{SV} = 14.3 \pm 0.1$ M^{-1}, which is a typical value for solvent-exposed chromophore groups. This means that the Trp residue of PDEγ is substantially solvated and accessible to the quencher molecules.

Hydrodynamic Properties of PDEγ (Gel-Filtration Experiments). To obtain information about the hydrodynamic di-

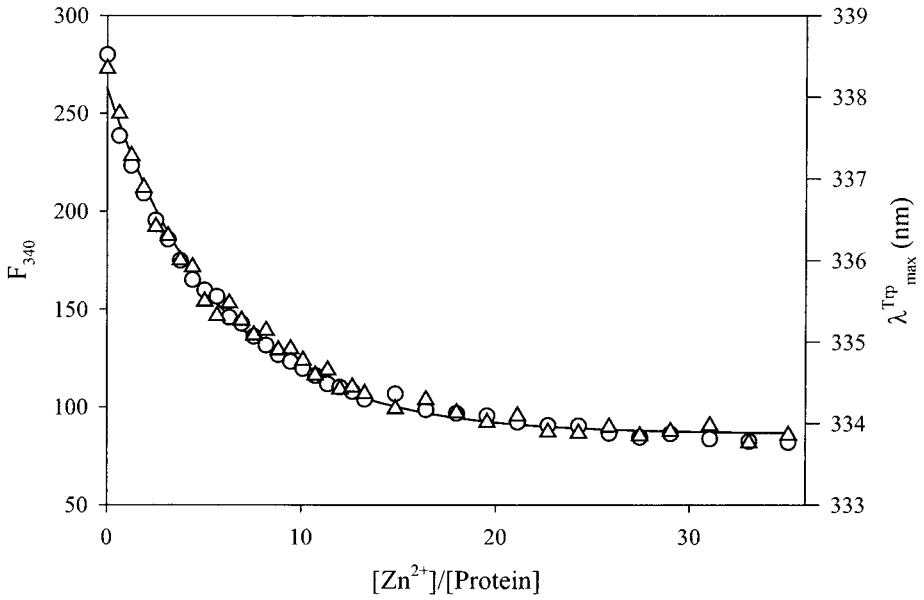

Figure 4. Spectrofluorometric Zn^{2+}-titration of PDEγ at 4 °C: triangles, position of the tryptophan fluorescence spectrum maximum; circles, fluorescence intensity at 340 nm (points are experimental; the curve is theoretical computed according to eq 3 and fitted to the experimental points). Protein concentration was 1 μM; 10 mM HEPES, pH 8.0. Fluorescence was excited at 280 nm.

mensions of PDEγ, the gel-filtration behavior of the protein under different experimental conditions was studied. Gel-permeation chromatography separates proteins by differences in their hydrodynamic dimensions rather than by their molecular masses.[19] This approach has been successfully applied to determine the Stokes radius values for proteins in different conformational states.[16,17,20,26] We have studied PDEγ by size-exclusion chromatography at neutral pH in the absence and in the presence of 8 M urea. Measurements were carried out at 15 °C using 0.1, 1.0, and 10.0 μM PDEg. In all cases, the gel-filtration profile contained a single symmetric elution peak. The position of this peak was used to calculate the R_S value (see the Experimental Section). We have established that independently on protein concentration the hydrodynamic dimensions of PDEγ at neutral pH are close to those measured in the presence of 8 M urea (R_S = 24.8 ± 0.8 and 29.1 ± 0.8 Å, respectively). Both values are very close to R_S calculated for a completely unfolded protein with a molecular mass of 9669 Da (R_S = 27.7 Å). Association did not affect the results of gel-filtration investigations, since they were independent of protein concentration within the wide range of PDEγ concentration (0.1−10.0 μM). Thus, under conditions of neutral pH and 15 °C and within the above-mentioned protein concentration range, PDEγ is essentially unfolded even in the absence of denaturant.

Effect of Temperature on PDEγ Intrinsic Fluorescence and Far-UV CD Spectrum. Figure 3A represents the temperature dependence of the far-UV CD and the intrinsic tryptophan fluorescence intensity measured for PDEγ at pH 8. One can see that the temperature rise is accompanied by a substantial and cooperative rearrangement of the protein structure, with the half-transition point in the vicinity of 21−23 °C. Interestingly, the temperature dependence of $[\theta]_{222}$ shows the heat-induced development of more ordered structure. Figure 1B represents additional confirmation of this conclusion. At higher temperatures, a considerable rearrangement of the spectrum is observed; in particular, the position of the major minimum is shifted to longer wavelengths, and a pronounced decrease of the trough at 200 nm is observed, accompanied by a considerable increase in negative ellipticity at 222 nm. Such far-UV CD spectral changes can be explained by the appearance of some elements of ordered secondary structures in the protein at high temperature.[27,28]

Interestingly, at the end of the temperature-induced transition (in the vicinity of 30 °C), the PDEγ molecule is still largely unfolded. The far-UV CD data are consistent with the assumption that an increase in temperature from 2 to 30 °C is accompanied by an increase in helical content of ∼5%. At the same time, these minor structural changes occur in a rather cooperative manner with the simultaneous change of all the parameters studied, indicative of a real structural transition between two ensembles of essentially disordered conformations.

Figure 3B illustrates the effect of temperature on static light scattering measured for the 1 μM PDEγ solution. It can be seen that the temperature course of this parameter is described by the sigmoidal curve, with a sharp 2.3-fold increase occurring within the temperature interval from 20 to 30 °C. Further temperature rise is accompanied by modest and gradual increase in the static light scattering. Interestingly, the half-transition point of this process (23 °C) coincides with that measured by changes in the intrinsic fluorescence and far-UV CD spectrum (21−23 °C). Thus, the results presented here are consistent with the assumption that temperature induces formation of partially folded PDEγ species, which tends to associate.

PDEγ Is a Zinc-Binding Protein. Mechanism of Zinc Binding. It was previously noted that PDEγ binds zinc cations.[9] Figure 2A shows that the interaction with zinc is accompanied by substantial changes in Trp fluorescence, providing an easy assay for monitoring the process. Figure 4 represents the results of a spectrofluorometric Zn^{2+}-titration of PDEγ at 4 °C showing the dependence of fluorescence intensity at 340 nm (circles) and fluorescence maximum position (squares) on zinc concentration. The increase in zinc concentration results in a ∼5 nm blue shift in λ_{max} and a substantial decrease in fluorescence intensity and fluorescence quantum yield. To avoid uncertainties connected with protein association, all Zn^{2+} titration

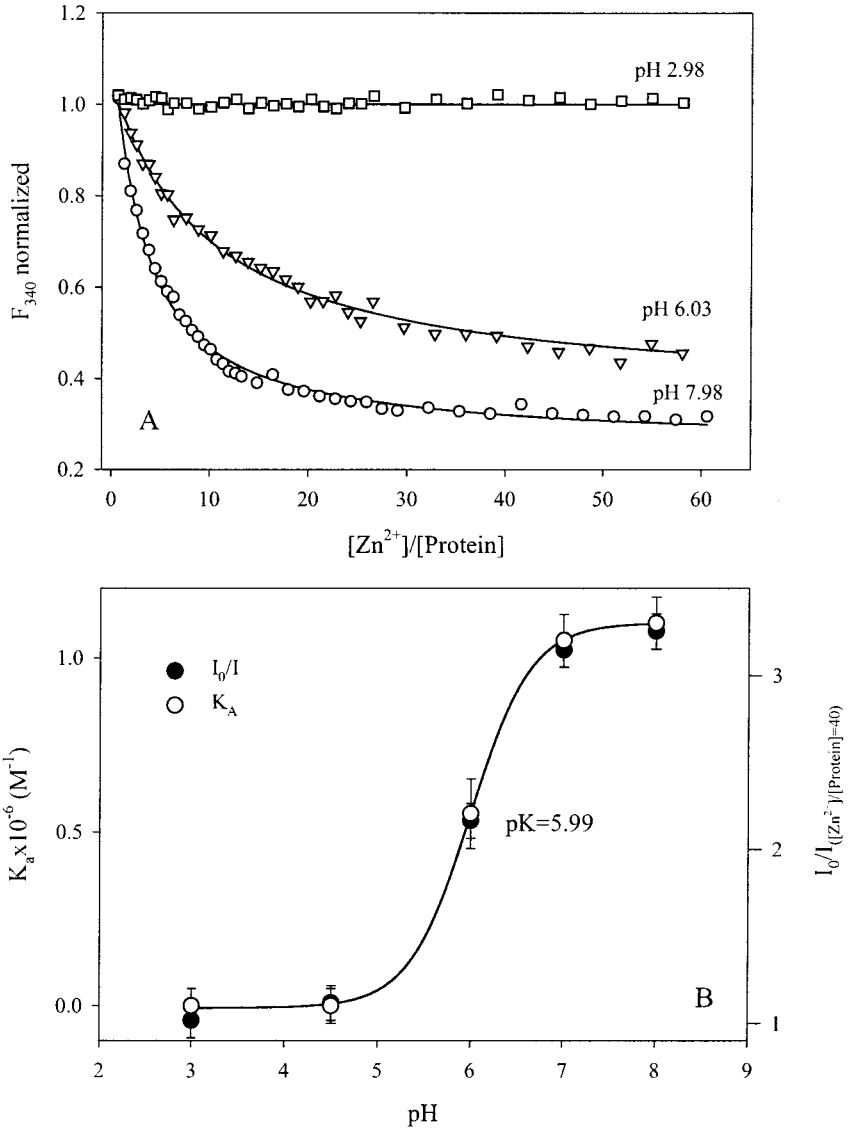

Figure 5. (A) Representative curves of the spectrofluorometric Zn^{2+} titration of PDEγ under conditions of different pH. Corresponding pH values are shown near the curves. (B) Effect of pH on zinc-binding capacity of PDEγ. The transition was monitored by pH-induced changes in association constant, K_a (open circles), and changes in the ratio I_o/I, where I_o and I are the fluorescence intensity in the absence or presence of 40 molar excess of zinc. Measurements were carried out at 4 °C. Protein concentration was 1 μM. Fluorescence was excited at 280 nm.

measurements were performed at 4 °C where protein was shown to be monomeric.

The experimental data presented in the Figure 4 were fitted by a theoretical curve computed according to the simplest one-site binding scheme:

$$\text{protein} + Zn^{2+} \overset{K}{\Leftrightarrow} \text{protein}\cdot Zn \qquad (6)$$

The best fit was achieved when $K = (1.09 \pm 0.09) \times 10^6\ M^{-1}$.

C-Terminal Histidines Are Involved in Zinc Binding. Figures 2A and 4 show that Zn^{2+}-binding is accompanied by considerable decrease in intrinsic fluorescence intensity and a blue shift in λ_{max}. This means that the environment of the Trp residue changes during the interaction of PDEγ with the cation, suggesting that some groups in the vicinity of this residue may participate in Zn^{2+} coordination. To understand which specific groups are involved in the zinc binding, spectrofluorometric Zn^{2+}-titrations of PDEγ were studied at 4 °C as a function of pH. Illustrative results of these studies are presented in Figure 5A. Both the shape and amplitude of the Zn^{2+} titration curve are very pH-dependent. The largest amplitude and highest sharpness of the titration curve were observed at neutral pH, in the vicinity of pH 6.0 both amplitude and sharpness decrease, and at more acidic pH the addition of zinc to the protein solution did not result in any spectral change. The pH profiles of the association constant and the relative decrease in the amplitude of the titration curve are presented in Figure 5B. The affinity of PDEγ to Zn^{2+} decreases dramatically with pH. [Note that the physiological pH in retina is assumed to be pH 7.3 (J.W. Lewis, personal communication). Thus, PDEγ possesses highest affinity to zinc under conditions of physiological pH.] Analysis of these data gives an apparent pK value of 6.0 (the half-transition point). The results suggest that the imidazole group(s) of histidine(s) could be involved in zinc binding since only the pK of imidazole is close to neutral pH. Analysis of the PDEγ amino acid sequence shows two his-

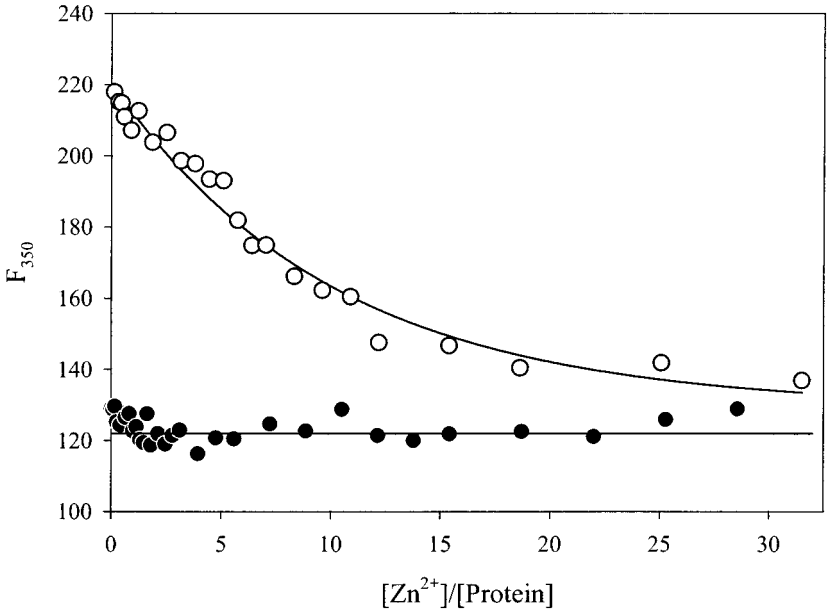

Figure 6. Spectrofluorometric Zn^{2+} titration of PDEγ fragments 1−72 (black circles) and 66−87 (open circles) monitored by changes in fluorescence intensity at 350 nm. Measurements were carried out at 5 °C. Protein concentration was 1 μM; 10 mM HEPES, pH 8.0. Fluorescence was excited at 280 nm.

tidines, His75 and His79, both in close vicinity to the single Trp70. This suggests that the C-terminal part of PDEγ is involved in the binding of Zn^{2+} under the conditions studied.

This suggestion was confirmed by investigation of the Zn^{2+} binding properties of different protein fragments. Figure 6 shows that the tryptophan fluorescence of PDEγ fragment 1−72 (without His 75 and His 79) does not respond to the addition of Zn^{2+} ions. On the other hand, the emission of PDEγ fragments 1−82, 58−87, and 66−87, all of which have the histidine residues, is sensitive to the addition of Zn^{2+}. Figure 6 illustrates data for the 66−87 fragment (open circles). The spectrofluorimetric analysis yields association constants of 9.3 $\times$ 10^5, 7.7 $\times$ 10^4, and 5.1 $\times$ 10^4 M for fragments 1−82, 58−87, and 66−87, respectively. This means that zinc binding requires the presence of the histidine residues, suggesting their direct coordination to the cation.

Structural Consequences of Zinc Binding to PDEγ. Figure 1A shows that the secondary structure of PDEγ is affected by the interaction with zinc, and at all conditions studied the Zn^{2+}-loaded protein exhibits more ordered secondary structure, compared to Zn^{2+}-free PDEγ. For example, at 4 °C the addition of 10-fold molar excess of Zn^{2+} to the protein solution induces structural perturbations similar to those observed for the Zn^{2+}-free protein at about 30 °C. Figures 2 and 4 show that Zn^{2+}-binding is accompanied by changes in the environment of the Trp residue. The spectrum of intrinsic fluorescence is blue shifted, consistent with burial of the Trp. Analysis of the acrylamide quenching (Figure 2B) confirms this conclusion, showing a notable decrease in accessibility of Trp to the quencher molecules (K_{SV} = 12.2 ± 0.1 M^{-1}).

Figure 7A compares the effect of temperature on the far-UV CD spectrum and fluorescence parameters of Zn^{2+}-loaded PDEγ. In this case, similarly to the Zn^{2+}-free protein (see Figure 3A), substantial and rather cooperative temperature-induced structural changes were observed, which were complete in the vicinity of 30 °C, leading to increased ordered secondary structure and compactness. The decrease in the accessibility of the Trp residue to acrylamide at 30 and 42 °C (K_{SV} = 9.3 ± 0.1 and 8.6 ± 0.1 M^{-1}, respectively (see also Figure 2B), suggests increased compactness at higher temperatures.

Figure 7B shows the temperature profile of the static light scattering measured for a 1 μM solution of Zn^{2+}-loaded PDEγ. In comparison with Zn^{2+}-free protein, this profile shows more complex behavior. In addition to a sigmoidal 2.2-fold increase in the static light scattering amplitude within the temperature interval from 20 to 30 °C, there is a pronounced (2.5-fold) subsequent increase in this parameter starting from 40 °C. This means that Zn^{2+}-loaded PDEγ is more prone to aggregate than Zn^{2+}-free protein. Importantly, the scattering profiles measured for Zn^{2+}-free and Zn^{2+}-loaded protein showed that in both cases PDEγ was most probably monomeric at low temperatures (cf. Figures 3B and 7B).

Interestingly, structural changes in both forms happen within the same temperature range. However, comparison of the temperature courses of Zn^{2+}-free and Zn^{2+}-loaded PDEγ (Figures 3 and 7) shows that the scale of structural changes undergone by the latter is much greater. Finally, as in the case of the temperature-induced reorganization of the Zn^{2+}-free protein, zinc-loaded PDEγ was still relatively disordered at the end of the temperature-induced transition (in the vicinity of 30 °C) and at higher temperatures (~60 °C). The far-UV CD data shows an increase from ~3% to ~10% in the helical content as the temperature rises from 4 to 60 °C. As seen in Figure 1A, even at 60 °C and 10 molar excess of Zn^{2+}, i.e., at the conditions where PDEγ adopts the most ordered conformation, it still lacks rigid tertiary structure.

Discussion

PDEγ Is a Natively Unfolded Zinc-Binding Protein. Possible Functional Implications. Our data show that at pH 8 and 4 °C the inhibitory subunit of phosphodiesterase (PDEγ) has little or no ordered secondary structure. The single Trp residue of this protein is substantially exposed to solvent, and the protein is characterized by hydrodynamic dimensions typical for the completely unfolded polypeptide of corresponding molecular

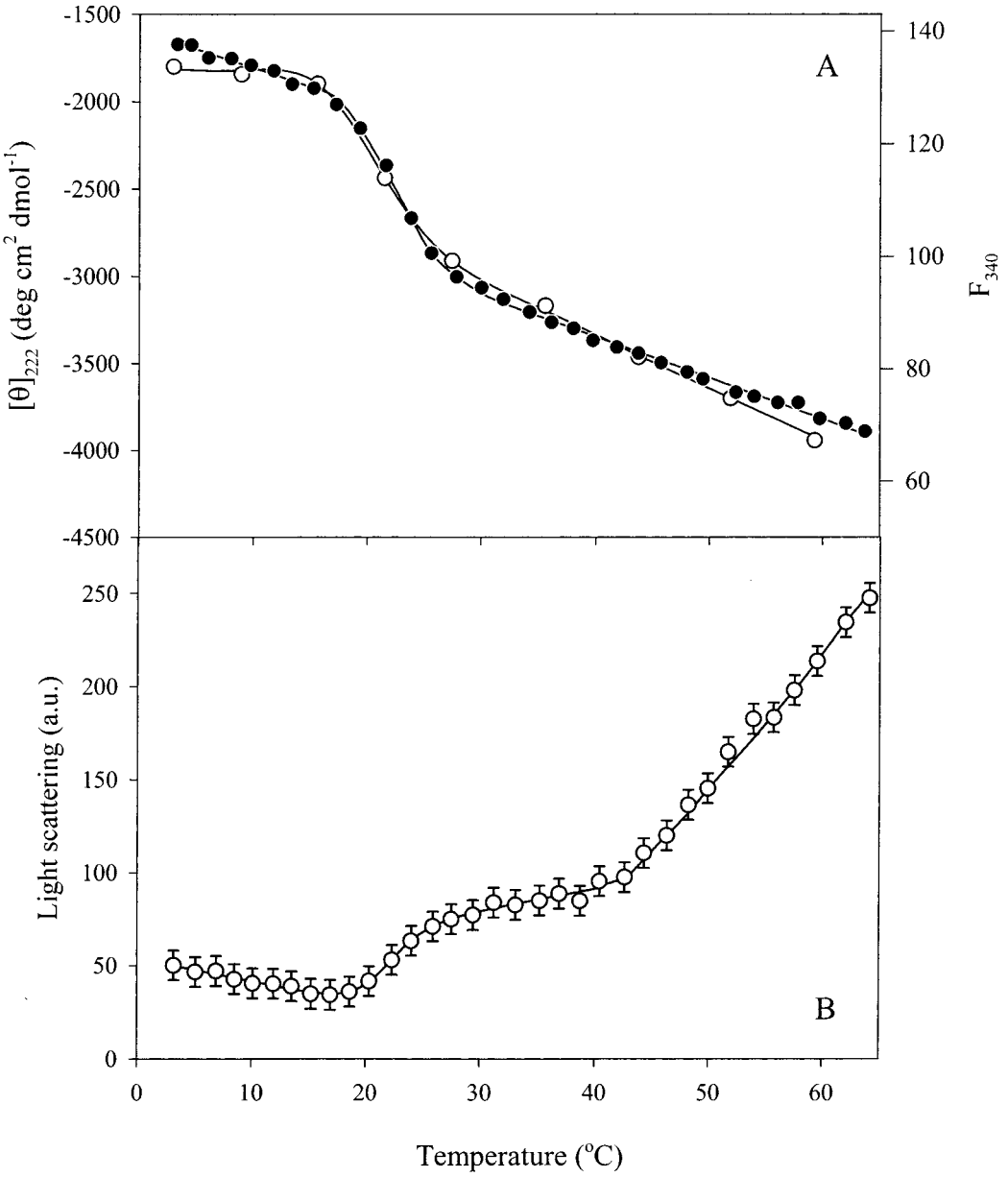

Figure 7. (A) Temperature-induced structural rearrangement of zinc-loaded PDEγ monitored by changes in the far-UV CD spectrum ($[\theta]_{222}$, circles) and intensity of Trp fluorescence spectrum (F_{340}, black circles). Protein concentration was 10 and 1 μM for CD and fluorescence measurements, respectively. (B) Temperature-induced association of zinc-loaded PDEγ monitored by changes in the static light scattering. Static light-scattering measurements were performed at 330 nm with the excitation at 330 nm. Protein concentration was 1 μM.

mass. This means that PDEγ belongs to the rapidly growing family of natively unfolded proteins. This conclusion explains some unusual structural properties of PDEγ reported in earlier studies. This includes high apparent molecular mass (~60kDa) of the purified protein,[29,30] high sensitivity of PDEγ to trypsinolysis,[31] and high resistance of this protein to the heating to 100 °C.[29,31,32]

PDEγ became somewhat more structured when the temperature was increased, showing a cooperative structural transition with T_m ~23 °C. However, the conformation of PDEγ remains substantially disordered even at the end of the temperature-induced transition. Structural properties of the temperature-modified PDEγ resembled those typical of globular proteins in their pre-molten globule state.[33−36] Very similar behavior has been described recently for another member of the natively unfolded family, human α-synuclein,[33−36] and several other intrinsically unstructured proteins.[39] Finally, our data showed that temperature-induced partial folding of the natively unfolded PDEγ might be accompanied by the association of pre-molten globule-like species.

We have shown here that PDEγ binds Zn^{2+}. The zinc-binding site is located within the C-terminal fragment of the protein, with His75 and His79 directly involved in coordination of the Zn^{2+}. Interaction with the cation induces minor structural rearrangement within the protein at low temperatures. Localization of the heat-induced transition is almost unaffected by the zinc binding. However, the Zn^{2+}-loaded protein shows a larger temperature-induced structural rearrangement. Thus, zinc could be considered to be a specific amplifier of the temperature-induced structural changes in PDEγ, which could be of functional importance.

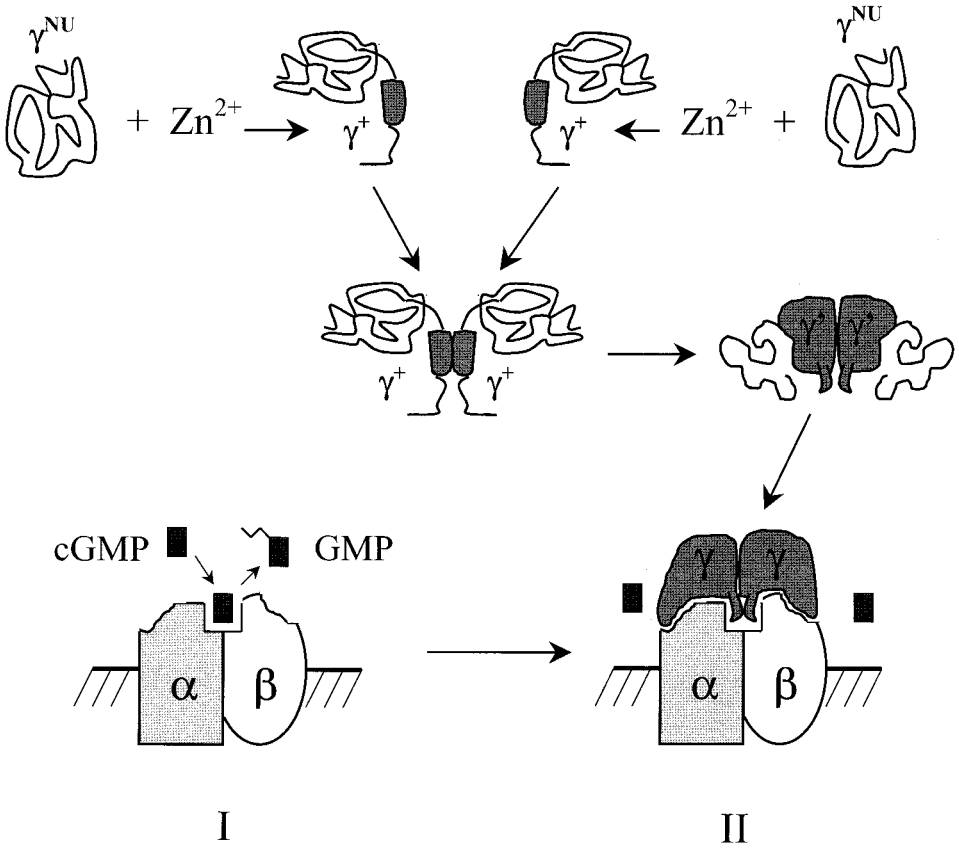

Figure 8. Model of zinc involvement in the regulation of the PDEγ interaction with the PDE catalytic complex. The process of cGMP hydrolysis by activated phosphodiesterase (α- and β-subunits) is presented as the transformation of the black rectangle into the rectangle with the tail. For further explanations, see the text.

The presence of high amounts of zinc in retina, indicating its essential role in this tissue, has been known for decades.[40] Unfortunately, information about free zinc concentration in photoreceptor outer segments is very restricted.[41] Nevertheless, the data on the total zinc content in photoreceptor outer segments from dark-adapted rat retina[41] indicate that outer segments possess about 0.5 mM of zinc. Since it has been shown that ocular tissues, the retina, in particular, contain relatively high concentrations of zinc,[5] several attempts to establish the role of this divalent cation in photoreceptor function have been undertaken. It has been shown that zinc co-purifies with rod outer segment proteins[6] and is a normal component of the disk membrane;[7] zinc, in a light-dependent manner, directly binds to purified rhodopsin (in its intradiscal part) and to disk membranes;[8] zinc deficiencies may be involved in photoreceptor degeneration;[42] zinc causes an apparent increase in rhodopsin phosphorylation;[43] 8-azido-[α-^{32}P]ATP binding to rhodopsin in rat rod outer segment preparations is higher in the presence of zinc.[44] These findings indicate a specific role of this cation in photoreceptor biochemistry. Attempts to find photoreceptor-specific protein(s) with affinity to zinc that could explain the effects of this cation in vision have identified some potential targets. These candidate proteins were retinol dehydrogenase,[7] carbonic anhydrase,[45] rhodopsin,[8] and PDE$\alpha\beta$.[46,47] We are now reporting another photoreceptor-specific protein, PDEγ, which also binds zinc and whose function could depend on the zinc concentration in the rod outer segment cytoplasm.

The K_d ($\sim$1 μM) that we determined for zinc binding to PDEγ is similar to the affinity estimated for other proteins known to bind and exchange this cation. Zinc has been shown to mediate the interaction between a hormone (prolactin) and its receptor:[48] K_d for zinc binding to this receptor (0.4 μM) is in the same range as the K_d found for bleached rhodopsin (1.4 μM[8]). Zinc is also known to have a procoagulant effect, and both fibrin and fibrinogen bind the cation with K_d values of 8−18 μM.[48] Albumin is probably responsible for transporting most of the zinc in plasma, and it has a binding constant of 0.1−0.2 μM for zinc.[49] On the other hand, the PDEγ affinity to Zn^{2+} reported here seems to be relatively weak when compared to many other zinc-binding proteins containing zinc fingers.[50] For example, a consensus zinc finger synthetic peptide exhibited a K_d for zinc of 2 pM.[51] Thus, the PDEγ affinity for this cation suggests that zinc could be involved in regulation of the visual cascade. This is quite likely by analogy to the role of another divalent cation, calcium, in photoreceptor biochemistry. Its compartmentalization within and outside rod cells and physiological significance have been extensively studied and could serve as a model for testing our zinc hypothesis.

It has been suggested that catalytic subunits of PDE isozymes are Zn^{2+} metalloenzymes, with the cation playing an important catalytic role in phosphodiester hydrolysis.[46] It has been shown that purified retinal rod cGMP phosphodiesterase PDE$\alpha\beta$ contained 3−4 mol of tightly bound zinc per protein heterodimer.[47] Moreover, removal of 93% of this tightly bound Zn^{2+} resulted in almost complete loss of protein activity, suggesting a catalytic, and probably stabilizing, role of this cation.[47] In agreement with this conclusion, substitution of serine for some histidine residues, proposed to act as ligands for catalytic Zn^{2+},

was found to abolish the catalytic activity of PDE4A,[52] and ^{65}-Zn^{2+} was found to bind to PDE4A and PDE5.[46,53]

Recently, it has been shown that brief incubation of PC12 cells with 150 μM Zn^{2+} lead to an essential almost 10-fold increase in the cellular cGMP level. This was attributed to the specific Zn^{2+}-induced inhibition of the cyclic nucleotide phosphodiesterase with an IC_{50} of about 13 μM.[54] Interestingly, during these experiments the total cellular zinc levels also increased from 2.87 $\pm$ 0.26 to 9.66 $\pm$ 2.45 μmol/mg protein.[54] We assume that this zinc uptake may be due to specific cation binding by the PDE inhibitory subunit. In fact, it has been shown that the catalytic heterodimer PDE$\alpha\beta$ is characterized by very high affinity to zinc ($K_d \sim 10$ nM),[47] assuming that it should be in zinc-saturated form even in the absence of exogenous Zn^{2+}. Specific cation binding to PDEγ may trigger structural transformation in this protein, leading to the enhancement of its inhibitory properties.

To understand the nature of these structural transformations, it would be important to compare the results of our in vitro studies of purified PDEγ with the structure of this protein bound to PDE$\alpha\beta$. Unfortunately, the crystal structure of the heterotetrameric cGMP phosphodiesterase has not yet been determined. In part, this could be due to problems connected with the crystallization of flexible PDEγ. In fact, it has been noted that PDEγ, being part of the PDE$\alpha\beta\gamma_2$ complex, is extremely sensitive to proteolysis by trypsin under conditions where the α and β subunits remain intact.[31,55] This means that the g subunit is flexible even when tightly bound to the catalytic heterodimer, as increased proteolytic degradation in vitro is a characteristic feature of proteins with high conformational flexibility.[14,56−58] On the other hand, it is known to be functional, and intrinsically unstructured proteins frequently (if not always) undergo pronounced disorder-to-order transitions.[13,14,39,58] The degree of these structural rearrangements varies over a very wide range, from coil-pre-molten globule transitions to formation of rigid ordered structures (reviewed in ref 58). Consequently, PDEγ is expected to be more rigid when complexed with PDE$\alpha\beta$ and/or transducin and/or other participants of the cGMP cascade of vision. In agreement with this conclusion, recent crystallographic studies revealed that the C-terminal half of PDEγ, PDEγ-46−87, adopts a relatively rigid structure when bound to the transducin α-subunit, Gtα, and the GTPase-activating protein regulator of G-protein signaling, RGS9.[59] These crystallographic data show that only 15 of 42 amino acid residues are involved into the formation of ordered secondary structure, giving rise to three short α-helixes, α_1 (PDEγ-63−66), α_2 (PDEγ-69−73), and α_3 (PDEγ-78−83).[59] On the basis of these data and on the results of Ala-scanning mutagenesis of the PDEγ-73−85 fragment, undertaken in order to identify point-to-point interactions between PDEγ and the PDE catalytic subunits, a model for the docking of PDEγ-50−87 to PDE$\alpha\beta$ has been suggested.[60] According to this model, formation of the PDE$\alpha\beta\gamma$ complex is accompanied by propagation of helix α_3 toward residue 75, giving rise to the helix α_3' (PDEγ-75−83) or perhaps even a continuous α-helix PDEγ-69−83.[60] Interestingly, His75 and His79 (which were shown in our study to be directly involved in the coordination of zinc) are four residues apart; i.e., their sequence localization resembles that of zinc-coordinating histidines in α-helical part of so-called zinc-finger domains.[61,62] This means that within helix α_3' (or the continuous α-helix PDEγ-69−83) side chains of His75 and His79 will have a spatial configuration favoring zinc coordination. We assume that interaction of natively unfolded PDEγ with zinc may induce the formation of helix α_3'/α-helix PDEγ-69−83 and, hence, lead to the stabilization of the active conformation of the PDE inhibitory subunit. Furthermore, zinc may be released from PDEγ during the activation of PDE catalytic subunits by transducin, as a consequence of essential structural rearrangements induced in PDEγ due to the interaction with Gtα.

Interestingly, our preliminary data indicate that zinc cations at sub-micromolar concentrations influence the biochemical properties of PDEγ, such as inhibition of trypsin activated PDE or PDE activation by transducin, studied in vitro similarly to the test systems described by Lipkin et al.[63] All this allows us to propose a model for zinc involvement in the regulation of the interaction of PDEγ with the PDE catalytic complex. This model is presented in Figure 8. **First Stage.** Activated phosphodiesterase (α- and β-subunits, PDE$\alpha\beta$) hydrolyze cGMP. Sites of PDEγ binding are located in the vicinity of the catalytic site. There is no effective inhibition of PDE by PDEγ because the inhibitory subunit is disordered and does not have appropriate structural elements to form a stable complex with PDE$\alpha\beta$. In parallel, the top line shows that in the presence of Zn^{2+} natively unfolded PDEγ, γ^{NU}, may undergo structural rearrangements in such a way that part of the protein becomes more structured due to interaction with zinc. This structured part is presumably located in the vicinity of C-terminus of PDEγ. However the last five C-terminal residues, to which the inhibitory activity is mapped, may not be involved into the structured fragment. As a result, PDEγ acquires a conformation γ^+ that, having higher propensity for self-assembly, forms dimers. As a result of dimerization, new structural rearrangements take place and PDEγ gains a conformation γ' that has high affinity for the specific binding sites located on PDE$\alpha\beta$. This brings us to the **second stage**. Here, Zn^{2+}-loaded PDEγ dimer forms a complex with PDE$\alpha\beta$ and inhibits activity of the latter due to the penetration of last five C-terminal residues into the active site and/or due to its simple steric blocking. Formation of the holoenzyme between two PDEγ molecules and the PDE catalytic complex is accompanied by new structural rearrangements within both inhibitory subunits, transforming them into a relatively tightly packed, folded conformation.

The basis underlying the assumption in the third stage is based on the following observations: (i) The propensity for self-association or aggregation is a general characteristic of non-native proteins.[21,64−75] (ii) The process of self-association can induce additional structure in a partially folded protein.[74−79] (iii) The conformation of PDEγ is protein concentration dependent. We have established that at high protein concentrations ($\sim$100 μM) PDEγ is characterized by a far-UV CD spectrum typical of a relatively folded protein (see spectrum presented by circles in Figure 1). (iv) Temperature induces association of partially folded PDEγ molecules, and the tendency to self-oligomerize is more pronounced in the presence of Zn^{2+} (see Figures 3B and 7B).

Clearly, further investigations are required to clarify the exact details of the involvement of zinc in the regulation of the vision photosystem.

Acknowledgment. We are very grateful to Prof. Vadim T. Ivanov for critical reading the manuscript and for kind and fruitful attention toward this work. This work was supported in part by RFBR (Russian Foundation for Basic Research) (Grant Nos. 98-04-48907 and 98-04-49211) and by a NATO Collabora-

tive Linkage Grant. The research of V.E.Z. was supported in part by an International Research Scholar's award from the Howard Hughes Medical Institute (Grant No. 75195-544203).

Abbreviations: cGMP, cyclic GMP; PDE, cGMP phosphodiesterase; PDE$\alpha\beta$, PDE catalytic subunits; PDEγ, cGMP phosphodiesterase γ-subunit; Gtα, rod G protein (tansducin) α-subunit; RGS9, GTPase-activating protein regulator of G-protein signaling; R_S, Stokes radius; CD, circular dichroism; UV, ultraviolet; *M*, molecular mass; N, native state; U, unfolded state; NU, natively unfolded; K_d, dissociation constant; K_{SV}, Stern−Volmer constant.

References

(1) Hofmann, K. P.; Heck, M. *Biomembranes* **1996**, *2*, 141−198.
(2) Ovchinnikov, Yu. A.; Lipkin, V. M.; Kumarev, V. P.; Gubanov, V. V.; Khramtsov, N. V.; Akhmedov, N. B.; Zagranichny, V. E.; Muradov, K. G. *FEBS Lett*. **1986**, *204*, 288−292.
(3) Kroll, S.; Phillips, W. J.; Cerione, R. A. *J. Biol. Chem*. **1989**, *264*, 4490−4497.
(4) Takemoto, D. J.; Cunnick, J. M. *Cellular Signaling* **1990**, *2*, 99−104.
(5) Vallee, B. L.; Falchuk, K. H. *Physiol. Rev*. **1993**, *73*, 79−118.
(6) Tam, S. W.; Wilber, K. E.; Wagner, F. W. *Biophys. Biochem. Res. Commun*. **1976**, *72*, 302−309.
(7) McCormick, L. D. *Biophys. J.* **1985**, *47*, 381−385.
(8) Shuster, T. A.; Nagy, A. K.; Conly, D. C.; Farber, D. B. *Biochem. J.* **1992**, *282*, 123−128.
(9) Rodionova, L. N.; Zagranichny, V. E.; Rodionov, I. L.; Lipkin, V. M.; Ivanov, V. T. *Russ. J. Bioorg. Chem*. **1997**, *23*, 823−838.
(10) Schweers, O.; Schönbrunn-Hanebeck, E.; Marx, A.; Mandelkow, E. *J. Biol. Chem*. **1994**, *269*, 24290−24297.
(11) Weinreb, P. H.; Zhen, W.; Poon, A. W.; Conway, K. A.; Lansbury, P. T., Jr. *Biochemistry* **1996**, *35*, 13709−13715.
(12) Uversky, V. N.; Gillespie, J. R.; Fink, A. L. *Proteins Struct. Funct. Genet.* **2000**, *42*, 415−327.
(13) Wright, P. E.; Dyson, H. J. *J. Mol. Biol.* **1999**, *293*, 321−331.
(14) Dunker, A. K.; Lawson, J. D.; Brown, C. J.; Williams, R. M.; Romero, P.; Oh, J. S.; Oldfield, C. J.; Campen, A. M.; Ratliff, C.; M.; Hipps, K. W.; Ausio, J.; Nissen, M. S.; Reeves, R.; Kang, C.-H.; Kissinger, C. R.; Bailey, R. W.; Griswold, M. D.; Chiu, W.; Garber, E. C.; Obradovic, A. *J. Mol. Graph. Model*. **2001**, *19*, 26−59.
(15) Arshavsky, V. Y.; Dumke, C. L.; Zhu, Y.; Artemyer, N. O.; Skiba, N. P.; Hamm, H. E.; Bownds, M. D. *J. Biol. Chem*. **1994**, *269*, 19882−19887.
(16) Corbett, R. J. T.; Roche, R. S. *Biochemistry* **1984**, *23*, 1888−1894.
(17) Uversky, V. N. *Biochemistry* **1993**, *32*, 13288−13298.
(18) Ackers, G. L. *J. Biol. Chem*. **1967**, *242*, 3237−3238.
(19) Ackers, G. L. *Adv. Protein Chem*. **1970**, *24*, 343−446.
(20) Uversky, V. N. *Int. J. Bio-Chromatogr.* **1994**, *1*, 103−114.
(21) Tanford, C. *Adv. Protein Chem*. **1968**, *23*, 121−282.
(22) Stryer, L. *Science* **1968**, *162*, 526−33.
(23) Permyakov, E. A. *Fluorescent Spectroscopy of Proteins*; CRC Press: Boca Raton, Ann Arbor, London, Tokyo, 1993.
(24) Eftink, M. R.; Ghiron, C. A. *Anal. Biochem*. **1981**, *114*, 199−227.
(25) Lakowicz, J. R. *Principles of Fluorescence Spectroscopy*; Plenum Press: New York, London, 1983.
(26) Uversky, V. N. *Biochemistry (Moscow)* **1999**, *64*, 250−266.
(27) Chen, Y.-H.; Yang, J. T.; Chau, K. H. *Biochemistry* **1974**, *13*, 3350−3359.
(28) Chou, P. Y.; Fasman, G. D. *Biochemistry* **1974**, *13*, 222−245.
(29) Dumler, I. L.; Etingof, R. N. *Biochim. Biophys. Acta* **1976**, *429*, 474−484.
(30) Yamazaki, A.; Bartucca, F.; Ting, A.; Bitensky, M. W. *Proc. Natl. Acad. Sci. U.S.A.* **1982**, *79*, 3701−3706.
(31) Hurley, J. B.; Stryer, L. *J. Biol. Chem*. **1982**, *257*, 11094−11099.
(32) Hurley, J. B. *Methods Enzymol.* **1982**, *81*, 542−547.
(33) Uversky, V. N.; Ptitsyn, O. B. *Biochemistry* **1994**, *33*, 2782−2791.
(34) Uversky, V. N.; Ptitsyn, O. B. *J. Mol. Biol.* **1996**, *255*, 215−228.
(35) Uversky, V. N. *Prot. Pept. Lett.* **1997**, *4*, 355−367.
(36) Uversky, V. N. *Biofizika (Moscow)* **1998**, *43*, 416−421.
(37) Uversky, V. N.; Li, J.; Fink, A. L. *J. Biol. Chem*. **2001**, *276*, 10737−10744.
(38) Li, J.; Uversky, V. N.; Fink, A. L. *Biochemistry* **2001**, *40*, 11604−11613.
(39) Uversky, V. N. *Eur. J. Biochem*. **2002**, *269*, 2−12.
(40) Leiner, M.; Leiner, G. *Biol. Zentralbl.* **1942**, *62*, 119−131.
(41) Ugarte, M.; Osborne, N. N. *Prog. Neurobiol.* **2001**, *64*, 219−249.
(42) Laure-duPree, A. E. *Invest. Ophthalmol. Vis. Sci.* **1981**, *21*, 1−9.
(43) Shuster, T. A.; Martin, F.; Nagy, A. K. *Curr. Eye Res.* **1996**, *15*, 1019−1024.
(44) Shuster, T. A.; Nagy, A. K.; Farber, D. B. *Exp. Eye Res.* **1988**, *46*, 475−484.
(45) Galin, M. A.; Nano, H. D.; Hall, T. *Invest. Ophthalmol.* **1962**, *1*, 142−148.
(46) Francis, S. H.; Colbran, J. L.; McAllister-Lucas, L. M.; Corbin, J. D. *J. Biol. Chem*. **1994**, *269*, 22477−22480.
(47) He, F.; Seryshev A. B.; Cowan, C. W.; Wensel, T. G. *J. Biol. Chem*. **2000**, *274*, 20572−20577.
(48) Cunningham, B. C.; Bass, S.; Fuh, G.; Wells, J. A. *Science* **1990**, *250*, 1709−1712.
(49) Marx, G. *Arch. Biochem. Biophys.* **1988**, *266*, 285−288.
(50) Schwabe, J. W. R.; Klug, A. *Nature Struct. Biol.* **1994**, *1*, 345−349.
(51) Krizek, B. A.; Amann, B. T.; Kilfoil, V. J.; Merkle, D. L.; Berg, J. M. *J. Am. Chem. Soc.* **1991**, *113*, 4518−4523.
(52) Omburo, G. A.; Jacobitz, S.; Torphy, T. J.; Colmanm R. W. *Cell Signaling* **1998**, *10*, 491−497.
(53) Percival, M. D.; Yeh, B.; Falgueyret, J. P. *Biochem. Biophys. Res. Commun.* **1997**, *241*, 175−180.
(54) Watjen, W.; Benters, J.; Haase, H.; Schwede, F.; Jastorff, B.; Beyersmann, D. *Toxicology* **2001**, *157*, 167−175.
(55) Hurley, J. B. *Annu. Rev. Physiol.* **1987**, *49*, 793−812.
(56) Markus, G. *Proc. Natl. Acad. Sci. U.S.A.* **1965**, *54*, 253−258.
(57) Fontana, A.; Polverino de Laureto, P.; De Philipps, V. In *Protein Stability and Stabilization*; van den Tweel, W., Harder, A., Buitelear M., Eds.; Elsevier Science, Amsterdam, 1993; pp 101−110.
(58) Uversky, V. N. *Protein Sci*. **2002**, *11*, in press.
(59) Slep, K. C.; Kercher, M. A.; He, W.; Cowan, C. W.; Wensel, T. G.; Sigler, P. B. *Nature* **2001**, *409*, 1071−1077.
(60) Granovsky, A. E.; Artemyev, N. O. *Biochemistry* **2001**, *40*, 13209−13215.
(61) Berg, J. M.; Shi, Y. *Science* **1996**, *271*, 1081−1085.
(62) Friesen, W. J.; Darby, M. K. *Nature Struct. Biol.* **1998**, *5*, 543−546.
(63) Lipkin, V. M.; Bondarenko, V. A.; Zagranichny, V. E.; Dobrynina, L. N.; Muradov, Kh. G.; Natochin, M. Yu. *Biochim. Biophys. Acta* **1993**, *1176*, 250−256.
(64) London, J.; Skrzynia, C.; Goldberg, M. E. *Eur. J. Biochem*. **1974**, *47*, 409−415.
(65) Clark, A. H.; Saunderson, D. H. P.; Sugget, A. *Int. J. Pept. Protein Res.* **1981**, *17*, 353−364.
(66) Mitraki, A.; King, J. *Biotechnology* **1989**, *7*, 690−697.
(67) De Young, L. R.; Fink, A. L.; Dill, K. *Acc. Chem. Res.* **1993**, *26*, 614−620.
(68) De Young, L. R.; Dill, K.; Fink, A. L. *Biochemistry* **1993**, *32*, 3877−3886.
(69) Eliezer, D.; Chiba, K.; Tsuruta, H.; Doniach, S.; Hodson, K. O.; Kihara, H. *Biophys. J.* **1993**, *65*, 912−917.
(70) Oberg, K.; Chrunyk, B. A.; Wetzel, R.; Fink, A. L. *Biochemistry* **1994**, *33*, 2628−2634.
(71) Fink, A. L. *Methods Mol. Biol*. **1995**, *40*, 343−360.
(72) Fink, A. L. *Annu. Rev. Biophys. Biomol. Struct*. **1995**, *24*, 495−522.
(73) Ptitsyn, O. B. *Adv. Protein Chem*. **1995**, *47*, 83−229.
(74) Uversky, V. N.; Fink, A. L. *Biochemistry (Moscow)* **1998**, *63*, 456−462.
(75) Uversky, V. N.; Fink, A. L. *Biochemistry (Moscow)* **1998**, *63*, 463−469.
(76) Uversky, V. N.; Segel, D. J.; Doniach, S.; Fink, A. L. *Proc. Natl. Acad. Sci. U.S.A.* **1998**, *95*, 5480−5483.
(77) Uversky, V. N.; Karnoup, A. S.; Khurana, R.; Segel, D. J.; Doniach, S.; Fink, A. L. *Protein Sci*. **1999**, *8*, 161−173.
(78) Kuznetsova, I. M.; Biktashev, A. G, Khaitlina, S.Yu.; Vassilenko, K. S.; Turoverov, K. K.; Uversky, V. N. *Biophys. J*. **1999**, *77*, 2788−2800.
(79) Kuznetsova, I. M.; Stepanenko, O. V.; Turoverov, K. K.; Zhu, L.; Zhou, J.-M.; Fink, A. L.; Uversky, V. N. *Biochim. Biophys. Acta* **2002**, in press.

PR0155127